Available online at www.sciencedirect.com
ScienceDirect
Journal of Power Sources 179 (2008) 532–540
JOURNAL OF POWER SOURCES
www.elsevier.com/locate/jpowsour

Pt-based electrocatalysts for polymer electrolyte membrane fuel cells prepared by supercritical deposition technique

Ayşe Bayrakçeken [a], Alevtina Smirnova [b], Usanee Kitkamthorn [b,1], Mark Aindow [b], Lemi Türker [c], İnci Eroğlu [a], Can Erkey [d,*]

[a] *Department of Chemical Engineering, Middle East Technical University, Ankara 06531, Turkey*
[b] *Department of Chemical, Materials and Biomolecular Engineering, and Institute of Materials Science, University of Connecticut, Storrs, CT 06269-3136, USA*
[c] *Department of Chemistry, Middle East Technical University, Ankara 06531, Turkey*
[d] *Department of Chemical and Biological Engineering, Koc University, 34450 Sariyer, Istanbul, Turkey*

Received 24 August 2007; received in revised form 11 December 2007; accepted 24 December 2007
Available online 4 January 2008

Abstract

Pt-based electrocatalysts were prepared on different carbon supports which are multiwall carbon nanotubes (MWCNTs), Vulcan XC 72R (VXR) and black pearl 2000 (BP2000) using a supercritical carbon dioxide ($scCO_2$) deposition technique. These catalysts were characterized by using X-ray diffraction (XRD), high-resolution transmission electron microscopy (HRTEM) and cyclic voltammetry (CV). XRD and HRTEM results demonstrated that the $scCO_2$ deposition technique enables a high surface area metal phase to be deposited, with the size of the Pt particles ranging from 1 to 2 nm. The electrochemical surface areas (ESAs) of the prepared electrocatalysts were compared to the surface areas of commercial ETEK Pt/C (10 wt% Pt) and Tanaka Pt/C (46.5 wt% Pt) catalysts. The CV data indicate that the ESAs of the prepared Pt/VXR and Pt/MWCNT catalysts are about three times larger than that of the commercial ETEK catalyst for similar (10 wt% Pt) loadings. Oxygen reduction activity was investigated by hydrodynamic voltammetry. From the slope of Koutecky–Levich plots, the average number of electrons transferred in the oxygen reduction reaction (ORR) was 3.5, 3.6 and 3.7 for Pt/BP2000, Pt/VXR and Pt/MWCNT, correspondingly, which indicated almost complete reduction of oxygen to water.

Keywords: Supercritical carbon dioxide deposition; Electrocatalyst; Carbon; Polymer electrolyte membrane fuel cell; Platinum

1. Introduction

A polymer electrolyte membrane fuel cell (PEMFC) contains a membrane electrode assembly (MEA) typically consisting of an ionically conducting polymeric membrane sandwiched between two electronically conducting electrodes. Typical electrodes for PEMFC applications are made of a gas diffusion layer (usually porous carbon paper or carbon cloth) supporting a layer of finely dispersed Pt on carbon catalyst. Platinum is the most extensively used metal in the anode and cathode electrodes of PEMFCs because of its high catalytic activity for both oxidation and reduction reactions [1]. The high cost of Pt is prohibitive for commercialization of PEMFCs and research efforts are directed to reduce the amount of platinum utilized by improving membrane electrode assembly preparation techniques [2–5] or structures of carbon-supported catalysts [6,7]. The activities of the catalysts depend on several parameters such as the catalyst preparation technique, the type of carbon support, properties of the precursor, accessibility of the metal on the support, and testing conditions.

In the past, several different methods were utilized to deposit platinum on different carbon supports; these include: impregnation-reduction [8] microemulsion-based synthesis [9] and ion exchange [10]. The carbon supports used included Vulcan XC 72 R (VXR) [11], multiwall carbon nanotube (MWCNT) [12,13], carbon aerogel [14], activated carbon [15], black pearl

* Corresponding author. Tel.: +90 2123381866; fax: +90 2123381548.
E-mail address: cerkey@ku.edu.tr (C. Erkey).
[1] Present address: School of Metallurgical Engineering, Suranaree University of Technology, Muang, Nakorn Ratchasima 30000, Thailand.

0378-7753/$ – see front matter © 2008 Published by Elsevier B.V.
doi:10.1016/j.jpowsour.2007.12.086

2000 (BP2000) [16] and carbon cryogel [17]. In all these techniques, the objective has been to decrease the average size of the Pt particles in order to increase the catalytic surface area per unit mass of Pt, and also to disperse the Pt particles uniformly on the support. Among these techniques, impregnation has some drawbacks such as agglomeration which results in higher particle sizes [18]. Moreover, in the microemulsion-based technique, removing the surfactant may be problematic [19].

Supercritical deposition is an alternative and promising way to prepare electrocatalysts. This process involves the dissolution of a metallic precursor in a supercritical fluid and the exposure of a porous support to the solution. After adsorption of the precursor on the support, the metallic precursor is converted to its metal form by chemical or thermal reduction. Using a supercritical fluid (SCF) as the processing medium for synthesis of electrocatalysts has many advantages which are directly related to the special properties of the SCFs. Properties of a SCF are different from those of ordinary liquids and gases and are tunable simply by changing the pressure and temperature. In particular, density and viscosity change drastically at conditions close to the critical point. Since fluid densities can approach or even exceed those of liquids, various SCFs are good solvents for a wide range of organic and organometallic compounds. Compared with conventional liquid solvents, high diffusivities in SCFs combined with their low viscosities result in enhanced mass transfer characteristics. The low surface tension of SCFs permits better penetration and wetting of pores than liquid solvents do. Among the SCFs, supercritical carbon dioxide ($scCO_2$), readily accessible with a T_c of 31 °C and a P_c of 7.38 MPa, is particularly attractive since it is abundant, inexpensive, nonflammable, nontoxic, environmentally benign and leaves no residue on the treated medium [20]. This promising catalyst preparation technique results in small particle sizes and homogeneous dispersions [21–24]. An additional advantage of this technique is the ability to thermodynamically control [25,26] the metal loading.

In this study, the $scCO_2$ deposition method was used to prepare Pt-based electrocatalysts on different carbon supports such as MWCNT, VXR and BP2000. The synthesized catalysts were compared with commercially available Pt/C-ETEK and Pt/C-Tanaka catalysts by means of X-ray diffraction (XRD), high-resolution transmission electron microscopy (HRTEM) and cyclic voltammetry (CV) measurements.

2. Experimental

2.1. Catalyst preparation and characterization

Carbon supports, VXR and BP2000 from Cabot International and MWCNT (i.d. = 1–3 nm, o.d. = 3–10 nm, L = 0.1–10 μm >90%) from Aldrich were impregnated with Pt using the $scCO_2$ deposition technique. Prior to impregnation all carbon supports were heat treated in a pyrolysis oven at 423 K for 4 h in N_2 (99.999%, Airgas) atmosphere. In this synthesis, dimethyl (cyclooctadiene) platinum(II) ($PtMe_2COD$) (99.9%) (STREM) was used as the Pt precursor.

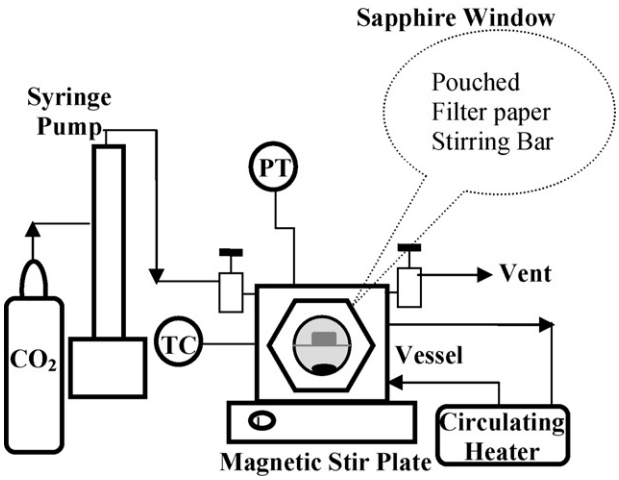

Fig. 1. Experimental setup for supercritical deposition.

A schematic of the supercritical deposition setup is given in Fig. 1. The deposition apparatus consists of a 54-ml custom-manufactured stainless steel vessel equipped with two sapphire windows, 25 mm in diameter, and sealed with poly(ether ether ketone) *O*-rings. A T-type thermocouple assembly (Omega Engineering, PX300-7.5KGV), a vent line and a rupture disk assembly (Autoclave Engineers) are also attached to the vessel.

The heat-treated carbon support was placed into a pouch made of a filter paper and placed into the vessel together with a certain amount of $PtMe_2COD$ precursor, and a stirring bar. For the desired metal loading, the amount of the $PtMe_2COD$ precursor was determined by using the adsorption isotherm of $PtMe_2COD$ onto the carbon support [22]. A stainless steel screen was used to separate the stirring bar from the filter paper pouch. The vessel was sealed and heated to 343 K using a circulating heater/cooler apparatus (Fisher Scientific Isotemp Refrigerated Circulator Model 80) and then charged slowly with carbon dioxide (99.998%, Airgas) to a pressure of 24.2 MPa using a syringe pump (ISCO, 260D). These conditions were maintained for a period of 6 h which was enough for the system to reach equilibrium and then the vessel was depressurized. After allowing the vessel to cool, the pouch was removed and the impregnated carbon support was weighed to determine the amount of precursor adsorbed using an analytical balance (Adventure Model Ar 2140) accurate to ±0.1 mg. Subsequently, the carbon support was placed in an alumina process tube in a tube furnace (Thermolyne 21100), and the precursor was reduced thermally under flowing N_2 (100 $cm^3\ min^{-1}$) for 4 h at 473 K.

The synthesized Pt/MWCNT (9.9%), Pt/BP2000 (47.5%) and Pt/VXR (9%) and commercially available Pt/C (ETEK, 10%) and Pt/C (Tanaka, 46.5%) catalysts were characterized by XRD and TEM in the as-synthesized condition with no subsequent cleaning or purification steps. XRD measurements were recorded by using a Cu Kα source in a SCINTAG XDS 2000 diffractometer. The diffractometer was operated in continuous scan mode at a scan rate of 0.6° min^{-1} in the range of 5–80° (2θ). HRTEM samples were produced by dispersing the material ultrasonically in ethanol, transferring a drop of this suspension onto a copper mesh grid coated with a holey carbon film, and

then allowing the ethanol to evaporate. The sample was examined in a UHR JEOL 2010 FasTEM operating at an accelerating voltage of 200 kV.

2.2. Electrochemical characterization

The electrochemical characterization of these catalysts was obtained by using cyclic voltammetry (CV). CV measurements were carried out in a standard three-electrode electrochemical cell. A silver–silver chloride electrode (Ag/AgCl, Cl^-) was used as the reference which was externally connected to the cell by a specially designed salt bridge filled with 0.1 M KCl solution and placed as close as possible to the working electrode to decrease the ohmic resistance. The possible leakage was checked by measuring the resistance of the salt bridge in 0.1 M KCl. The obtained value of 100 kΩ ensured the absence of leakage into the $HClO_4$ solution during the 2–3 h necessary to complete the experiment. Pt wire and a glassy carbon (GC) electrode (5 mm in diameter) were used as counter and working electrodes, respectively. Catalyst solutions were prepared by mixing measured amounts of either the commercial or the synthesized catalysts with 1 ml deionized water, 1 ml 1,2-propandiol and 400 μl 5% 5 wt% Nafion solution (Ion Solutions Inc.). The amount of the catalyst in solution was in the range of 22–25 mg, which correlates to the Pt loading in the support. In all experiments the catalyst loading on the GC electrode was set to 28 μg Pt cm^{-2}. The suspension was homogenized for 1 h using an Ultra-Turrax® T25 homogenizer followed by deposition of 5.8 μl of this solution onto the GC electrode and overnight drying.

CV data were collected in a 0.1 M $HClO_4$ electrolyte saturated with hydrogen for 30 min to remove the oxygen. Prior to the experiments the hydrogen supply tube was taken out of the solution and placed on the top of the electrolyte solution. All the experiments were performed at room temperature. After 10 cycles between 0.0 and 0.8 V at a scan rate of 50 mV s^{-1} the stabilized CV curves were recorded. In all the figures CV data are given with respect to normal hydrogen electrode (NHE). For hydrodynamic voltammograms, the electrolyte was saturated with oxygen for 30 min and the rotation speed was between 100 and 2500 rpm. The CV results were recorded in the range of 0–0.8 V at a scan rate of 10 mV s^{-1} in order to prevent the oxidation of the carbon support that usually occurs at 1.2 V [27]. Calculation of electrochemical surface area (ESA) was performed by using the area under the reduction part of the curve according to the equation published elsewhere [28].

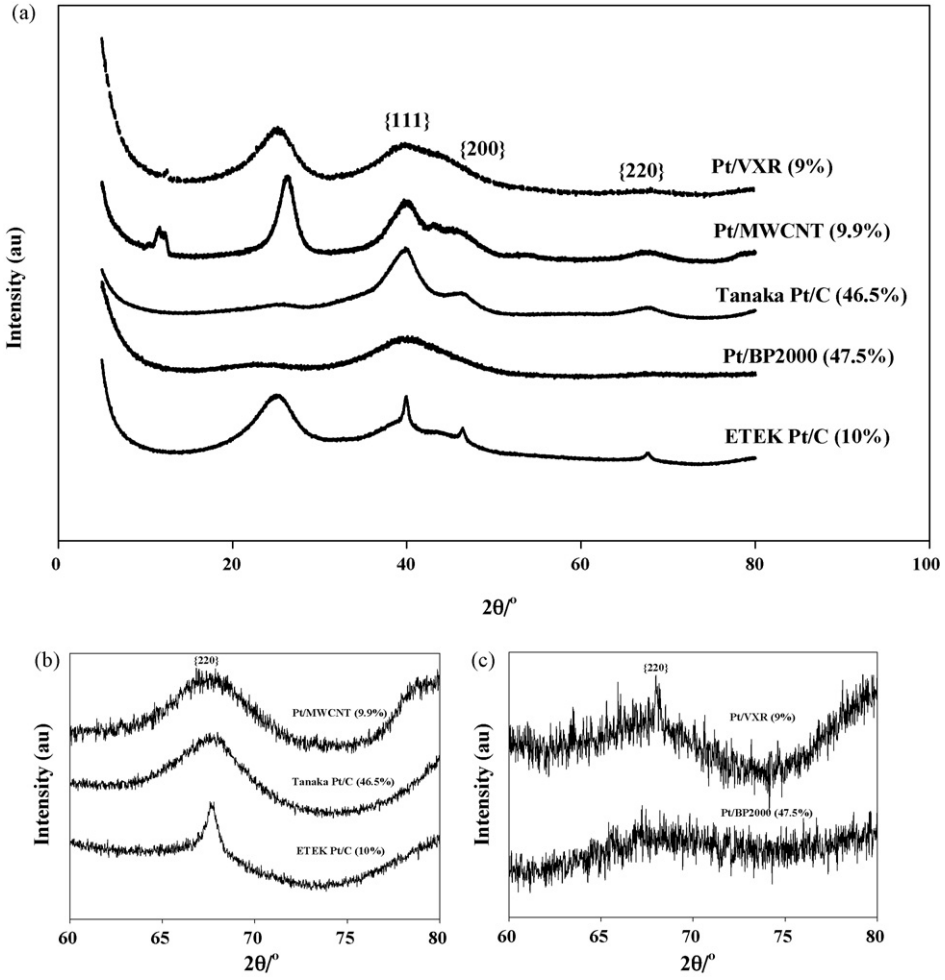

Fig. 2. (a) XRD patterns for the synthesized and commercial catalysts. (b) Narrow scan XRD pattern for ETEK Pt/C, Tanaka Pt/C and Pt/MWCNT catalysts. (c) Narrow scan XRD pattern for Pt/VXR and Pt/BP2000.

3. Results and discussion

The carbon supports used in this study were VXR, BP2000 and MWCNT which have total surface areas of 235 [8], 1450 [29] and 300 (Aldrich) $m^2\ g^{-1}$, respectively.

The XRD spectra for the prepared and commercial catalysts are presented in Fig. 2(a). For all catalysts the characteristic {1 1 1}, {2 0 0}, {2 2 0} peaks for face-centered cubic (fcc) Pt were obtained. Because the {1 1 1}, and {2 0 0} Pt peaks overlapped the broad C peaks, the sizes of the Pt particles were calculated from the Scherrer equation using the half full width at half maximum of the {2 2 0} reflection [30]. High-resolution XRD spectra obtained over the range $2\theta = 60–80^\circ$ from the catalysts ETEK Pt/C, Tanaka Pt/C, Pt/MWCNT and Pt/BP2000, Pt/VXR are given in Fig. 2(b) and (c), respectively. The equivalent surface area (SA) of the metal phase (Pt) was determined using the mean particle sizes obtained from the XRD data [31]. The mean particle sizes are given in Table 1 and indicate that highly dispersed Pt catalysts with small Pt particle sizes were obtained by using the $scCO_2$ deposition method.

HRTEM images obtained from the synthesized and commercial catalysts are presented in Fig. 3 for Pt/MWCNT (a), (b); Pt/VXR (c), (d); Pt/BP2000 (e), (f) and ETEK Pt/C (g)–(j). In agreement with XRD data, it can be seen that a small Pt particle size of about 1–2 nm and uniform Pt distribution can be achieved using the $scCO_2$ deposition method. From the literature [32] and the ETEK company data the size of the Pt particles of ETEK Pt/C (10 wt%) catalyst was around 2–3 nm. However, the calculations based on the XRD data gave a particle size of close to 6 nm. The reason for this discrepancy is that there is a broad Pt particle size distribution in the ETEK catalyst as shown by the TEM data presented in Fig. 3(g)–(j). On the contrary, there is a good agreement between XRD and TEM data for the samples synthesized by the $scCO_2$ deposition technique, indicating that they have a very narrow particle size distribution.

Among the carbon supports, the BP2000 has the highest surface area and it is this support on which the highest Pt loading was achieved in this work (47.5%). This is due to highest uptake of the Pt precursor due to the highest surface area. However, for the Pt/BP2000 catalysts that have different Pt loadings, the ESA values obtained were approximately the same, presumably due to similar size of the Pt particles (≈1 nm in diameter) which was confirmed by the XRD measurements.

CV results for the Pt/BP2000 catalysts which have 29 and 47.5 wt% Pt loadings are given in Fig. 4. The catalytic activity of these catalysts are very similar despite substantially different loadings. As demonstrated by the CV data in Fig. 5, the catalytic activity of the Pt/VXR prepared by supercritical deposition for electro-oxidation and reduction of hydrogen is substantially higher than the catalytic activity of commercial Pt/VXR. Among the three different supports utilized in supercritical deposition, VXR has the highest catalytic activity.

The calculated surface area and electrochemical surface area parameters are given in Table 1. Although Pt/VXR ($scCO_2$) has the highest ESA and a low particle diameter (Table 1), the Pt utilization is only 74%. It can be assumed that in the case of small (∼1 nm) Pt particles, the accessibility of the metal particles even in liquid electrolyte is more critical due to the partially hydrophobic nature of the carbon support. For Pt/MWCNT ($scCO_2$) and Pt/C (Tanaka), which have larger Pt particles (2 nm), the utilization of Pt seems to be higher.

The ESA values for the Pt/BP2000 catalysts which have 29 and 47.5 wt% Pt loadings are 110 and 102 $m^2\ g^{-1}$, respectively. Similar ESA values at substantially different loadings indicate that ESAs are primarily governed by the platinum particle size for the same support. Even though the particle size of Pt on VXR and BP2000 is approximately the same, the ESA of Pt/VXR is higher which results in a large difference in the Pt utilization for these two materials (Table 1). This could be due to differences in the structures of the carbon supports for these two catalysts, namely by the higher micropore volume of BP2000. Some of the platinum nanoparticles may be residing in the micropores and the electrolyte may not be contacting these particles. The Pt utilization value of over 100% in the case of Pt/C (ETEK) presumably arises because the Pt particle size is not uniform, as revealed in the HRTEM images from this material (Fig. 3(g)–(j)). We note, however, that Pt utilization values of over 100% have been reported elsewhere for ETEK Pt/C (20%) catalyst [33].

CV positive scans for O_2 reduction with rotation speeds varying between 100 and 2500 rpm at a 10 mV s^{-1} sweep rate for the synthesized Pt/VXR, Pt/MWCNT and Pt/BP2000 catalysts are presented in Figs. 6–8, respectively. The CV data show similar trends to the ESA data. Thus, for Pt/MWCNT and Pt/VXR the current is higher than that for Pt/BP2000, and in all three cases the current increases gradually with the speed of rotation. The limiting current plateaus obtained for Pt/VXR and Pt/MWCNT indicate that the oxygen reduction is fast enough at high overpotentials and follows a trend [33] similar to Pt/BP2000. If the electro-catalytically active sites are not distributed uniformly and the electrocatalytic reaction is slow, the current plateau becomes more inclined [34].

Table 1
Electrochemical and total surface area of the prepared and commercial catalysts

Catalyst	d (nm)[a]	SA_{Pt} ($m^2\ g^{-1}$)	ESA_{Pt} ($m^2\ g^{-1}$)	Pt wt%	% Pt utilization (ESA/SA × 100)
Pt/C (ETEK)	6	46.73	57	10	122
Pt/VXR ($scCO_2$)	1.2	233.64	173	9	74
Pt/MWCNT ($scCO_2$)	2	140.2	130	9.9	93
Pt/BP2000 ($scCO_2$)	1	280.4	102	47.5	36
Pt/C (Tanaka)	2	140.2	128	46.5	91

[a] From XRD data.

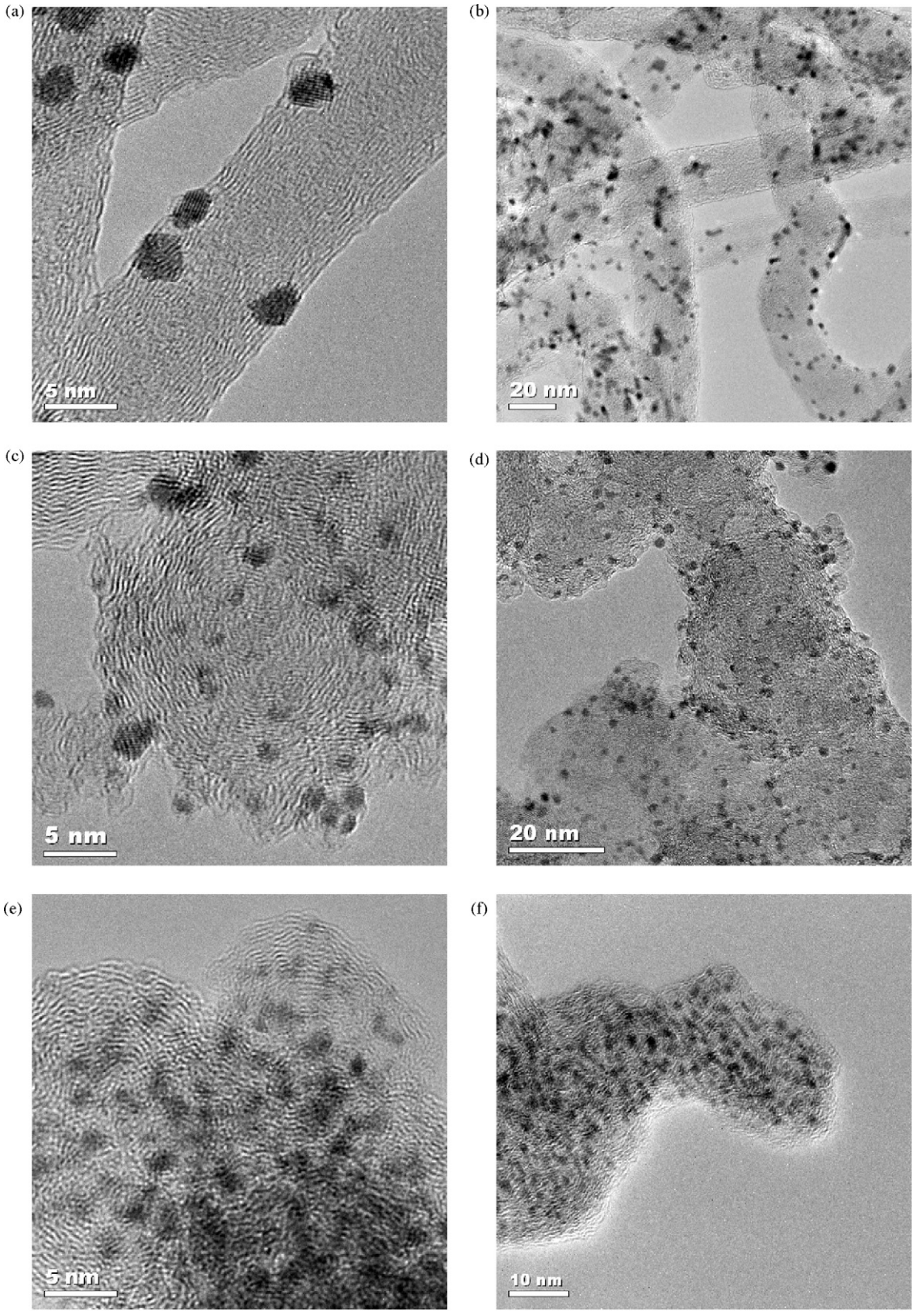

Fig. 3. HRTEM images for (a), (b) Pt/MWCNT; (c), (d) Pt/VXR; (e), (f) Pt/BP2000; (g)–(j) Pt/C (ETEK).

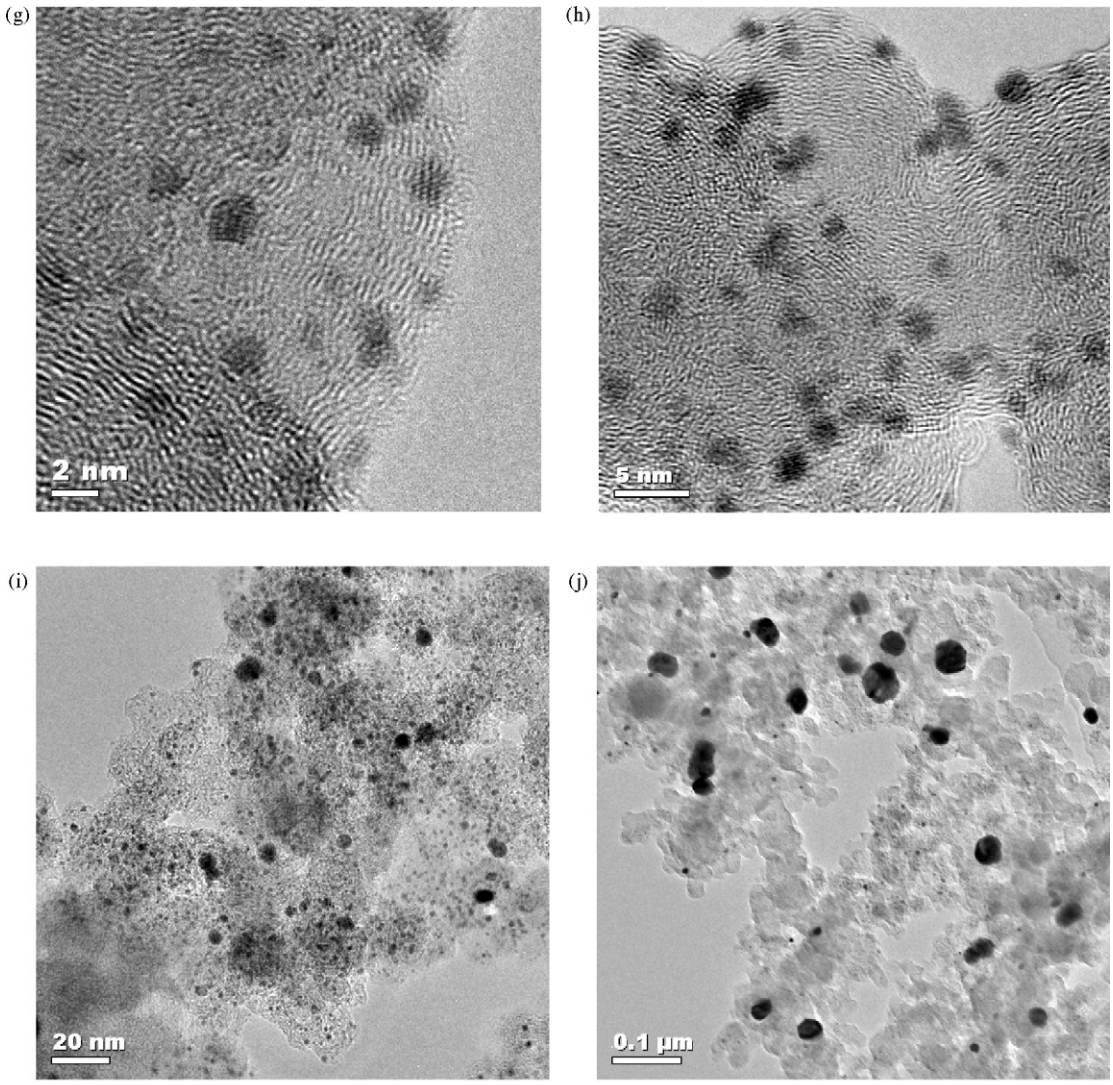

Fig. 3. (*Continued*).

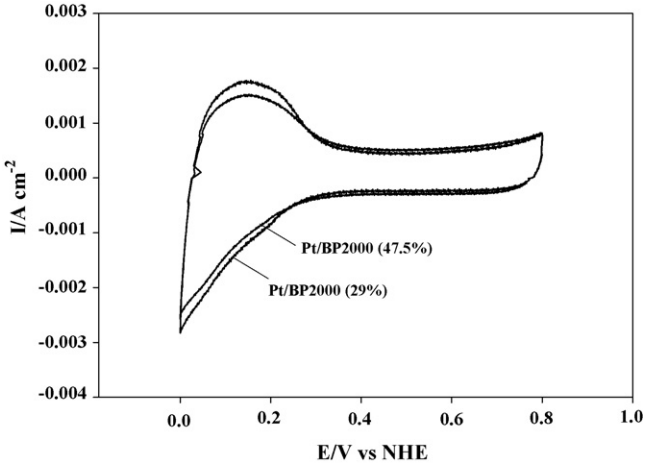

Fig. 4. CV results for Pt/BP2000 catalysts with different Pt loadings.

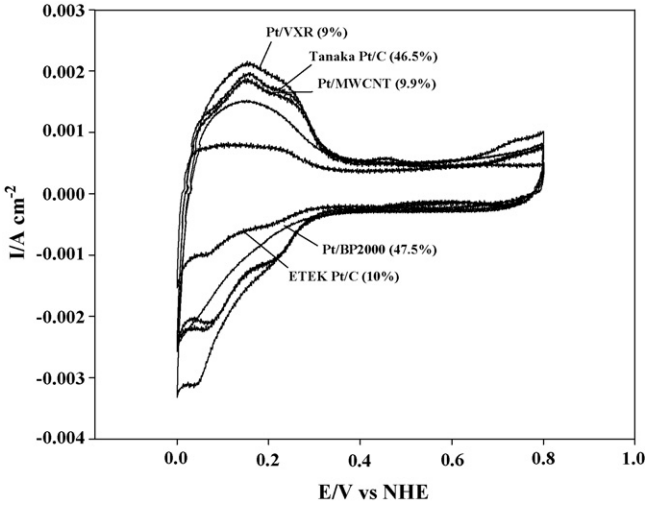

Fig. 5. Cyclic voltammogram for the synthesized catalysts in 0.1 M $HClO_4$ in H_2 atmosphere at a scan rate of 50 mV s^{-1}.

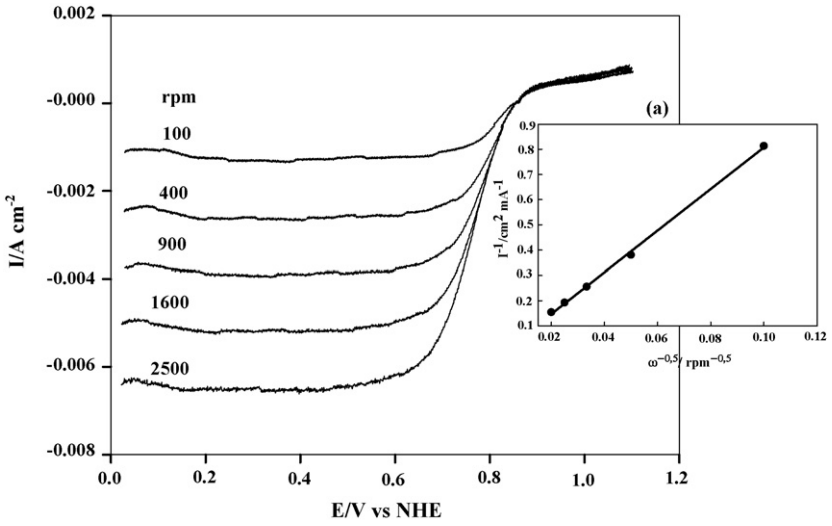

Fig. 6. Hydrodynamic voltammograms of positive scans of Pt/VXR for O_2 reduction in O_2 saturated 0.1 M $HClO_4$ (a) Koutecky–Levich plot at 0.2 V.

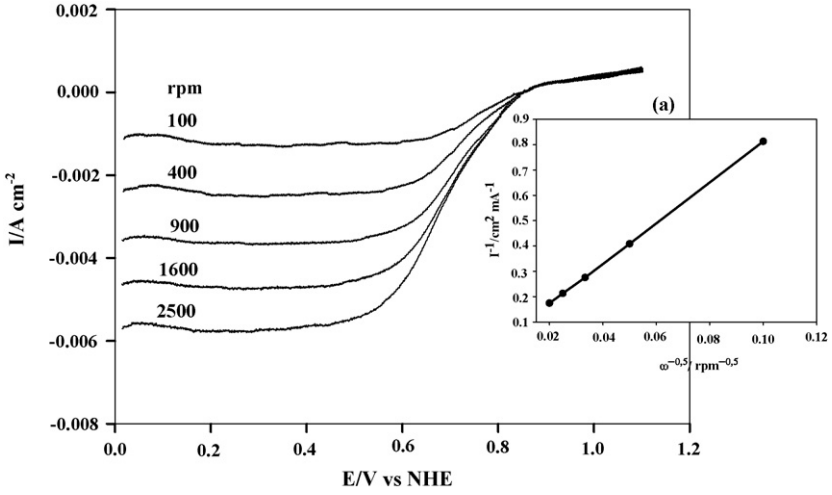

Fig. 7. Hydrodynamic voltammograms of positive scans of Pt/MWCNT for O_2 reduction in O_2 saturated 0.1 M $HClO_4$ (a) Koutecky–Levich plot at 0.2 V.

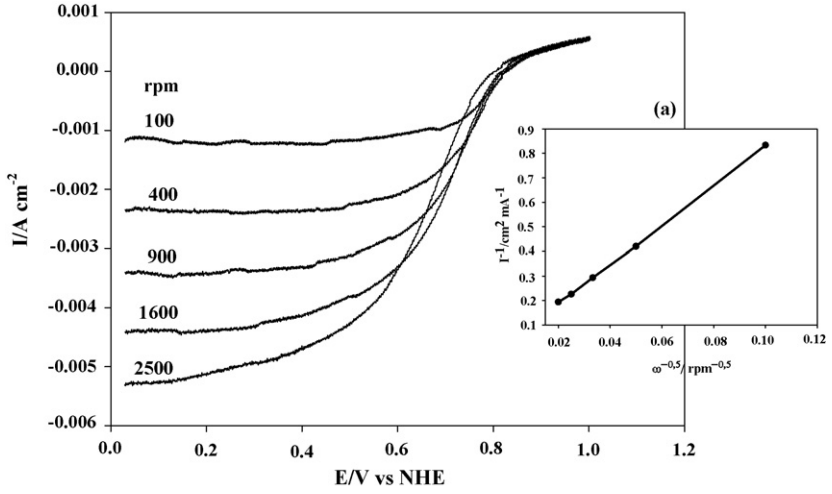

Fig. 8. Hydrodynamic voltammograms of positive scans of Pt/BP2000 for O_2 reduction in O_2 saturated 0.1 M $HClO_4$ (a) Koutecky–Levich plot at 0.2 V.

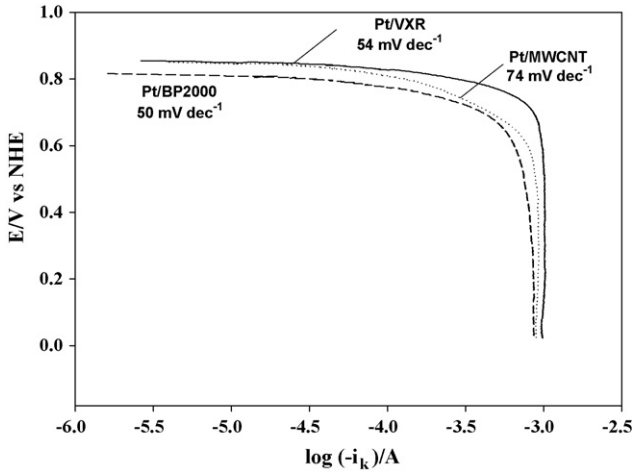

Fig. 9. Tafel plots of i_k for O_2 reduction in positive scans for synthesized catalysts in O_2 saturated 0.1 M $HClO_4$ for intermediate segment (0.85–0.75 V).

Koutecky–Levich plots were obtained by using Eq. (2) and plotting i^{-1} vs. $w^{1/2}$ [35].

$$\frac{1}{i} = \frac{1}{Bw^{1/2}} + \frac{1}{i_k} \tag{2}$$

The plots for Pt/VXR, Pt/MWCNT and Pt/BP2000 are presented in Figs. 6(a), 7(a) and 8(a), respectively. The linearity of the plots indicates that the rotation speeds used in this study are large enough that the number of electrons transferred per oxygen molecule (n) is independent of rotation speed. The Levich constants (B) obtained from the slope of the Koutecky–Levich plots, were used to calculate the number of electrons transferred per O_2 molecule (3) when w is expressed in revolutions per minute [36,37] using the following equation:

$$B = 0.2nFc_oD^{2/3}\nu^{-1/6} \tag{3}$$

where n is the number of electrons per O_2 molecule, F is the Faraday constant (96,485 C mol^{-1}), c_o is the oxygen bulk concentration (1.18×10^{-6} mol cm^{-3}) [38], D is the oxygen diffusion coefficient (1.9×10^{-5} cm^2 s^{-1}) [39], and ν is the viscosity of the electrolyte (9.87×10^{-3} cm^2 s^{-1}) [40]. By using the Levich constant obtained and Eq. (3), the number of electrons transferred was calculated as 3.5, 3.6 and 3.7 for Pt/BP2000 (1 nm), Pt/VXR (1.2 nm) and Pt/MWCNT (2 nm), respectively.

The oxygen reduction reaction is a multi-electron reaction which includes several elementary steps [41] and can follow either the $2e^-$ or $4e^-$ pathway, which leads to hydrogen peroxide formation or complete water formation reactions, respectively. The high number of electrons transferred per O_2 molecule calculated here (close to 4) is an indication of low H_2O_2 formation and an almost complete reduction of O_2 to H_2O.

The Tafel plots of kinetic currents (i_k) for oxygen reduction in positive sweep rates for the synthesized catalysts (Fig. 9) show the same order as the ESA values, i.e. Pt/VXR > Pt/MWCNT > Pt/BP2000. For high potentials and low potentials, Tafel slopes were reported as 60 and 120 mV $dec^{(1}$ for carbon-supported platinum catalysts, respectively [42]. However, there is a wide range of Tafel slopes reported in the literature for low potentials ranging between 120 and 200 mV $dec^{(1}$ [43]. The higher values of Tafel slopes are possibly due to low oxygen concentrations and due to a mixed activation/mass transport control [44]. The Tafel slopes obtained for the low overpotential and intermediate segment regions for Pt/MWCNT, Pt/VXR and Pt/BP2000 were 44, 36 and 40 mV $dec^{(1}$; and 74, 54 and 50 mV $dec^{(1}$, respectively. The Tafel slopes close to 40 mV $dec^{(1}$ in the low overpotential region indicate the dominance of the reduction of surface oxygen to OH. The Tafel slopes close to 70 mV $dec^{(1}$ in the intermediate region indicate that the oxygen reduction reaction kinetics can be explained with a mechanism of four electron transfer pathway involving a single electron transfer step yielding adsorbed O-containing species under Temkin adsorption conditions as the rate determining step [45].

4. Conclusion

The supercritical carbon dioxide deposition technique was used to prepare platinum nanoparticles on different carbon supports including VXR, MWCNT and BP2000. By using this method Pt nanoparticles, about 1–2 nm in diameter, were dispersed uniformly on the carbon supports. The electrochemical surface area and the activity for the oxygen reduction reaction were investigated by using rotating disk electrode experiments. The Pt/VXR catalyst prepared by supercritical deposition showed the best performance for electro-oxidation and hydrogen reduction and the electrocatalytic activity was substantially higher than the commercial Pt/VXR. Depending on the carbon support used, the electrochemical surface areas and the Pt utilizations changed, likely due to the different microporous and meso/macroporous structures of the supports that affect the accessibility of the electrolyte to the metal.

From CV data the number of electrons transferred per oxygen molecule was calculated as 3.5, 3.6 and 3.7 for Pt/BP2000, Pt/VXR and Pt/MWCNT, respectively. These values indicate that the oxygen reduction reaction is close to the $4e^-$ pathway, which results in an almost complete water formation reaction and negligible hydrogen peroxide formation. The Tafel slopes obtained for low overpotential and intermediate segment regions for Pt/MWCNT, Pt/VXR and Pt/BP2000 catalysts were 44, 36 and 40 mV $dec^{(1}$; and 74, 54 and 50 mV $dec^{(1}$, respectively.

Acknowledgment

The authors acknowledge financial support of Nigel Sammes and Molter Trent from the Connecticut Global fuel cell Center, UConn, USA, in purchasing the equipment.

References

[1] P. Costamagna, S. Srinivasan, J. Power Sources 102 (2001) 242–252.
[2] T. Nakakubo, S. Masaaki, K. Yasuda, J. Electrochem. Soc. 152 (2005) A2316–A2322.
[3] R. Benitez, J. Soler, L. Daza, J. Power Sources 151 (2005) 108–113.
[4] L. Xiong, A. Manthiram, Electrochim. Acta 50 (2005) 3200–3204.
[5] H. Kim, N.P. Subramanian, B.N. Popov, J. Power Sources 138 (2004) 14–24.

[6] T. Kawaguchi, W. Sugimoto, Y. Murakami, Y. Takasu, J. Catal. 229 (2005) 176–184.
[7] Z. Zhou, W. Zhou, S. Wang, G. Wang, L. Jiang, H. Li, G. Sun, Q. Xin, Catal. Today 93 (2004) 523–528.
[8] J. Zhang, X. Wang, C. Wu, H. Wang, B. Yi, H. Zhang, React. Kinet. Catal. Lett. 83 (2004) 229–236.
[9] M.J. Escudero, E. Hontañón, S. Schwartz, B. Boutonnet, L. Daza, J. Power Sources 106 (2002) 206–214.
[10] Y. Shao, G. Yin, J. Wang, Y. Gao, P. Shi, J. Power Sources 161 (2006) 47–53.
[11] V. Raghuveer, A. Manthiram, Electrochem. Solid-State Lett. 7 (2004) A336–A339.
[12] Z. Liu, X. Lin, J.Y. Lee, W. Zhang, M. Han, L.M. Gan, Langmuir 18. (2002) 4054–4060.
[13] W. Li, C. Liang, W. Zhou, J. Qiu, Z. Zhou, G. Sun, Q. Xin, J. Phys. Chem. B 107 (2003) 6292–6299.
[14] J. Marie, S. Berthon-Fabry, P. Achard, M. Chatenet, A. Pradourat, E. Chainet, J. Non-Crystal. Solids 350 (2004) 88–96.
[15] J. Maruyama, I. Abe, Electrochim. Acta 48 (2003) 1443–1450.
[16] K. Amine, K. Yasuda, H. Takenaka, Ann. Chim. Sci. Mat. 23 (1998) 331–335.
[17] B.M. Babić, Lj.M. Vračar, V. Radmilović, N.V. Krstajić, Electrochim. Acta 51 (2005) 3820–3826.
[18] C.L. Hui, X.G. Li, I.M. Hsing, Electrochim. Acta 51 (2005) 711–719.
[19] K.M.K. Yu, C.M.Y. Yeung, D. Thompsett, S.C. Tsang, J. Phys. Chem. B 107 (2003) 4515–4526.
[20] Y. Zhang, C. Erkey, J. Supercrit. Fluids 38 (2006) 252–267.
[21] A. Bayrakceken, U. Kitkamthorn, M. Aindow, C. Erkey, Scr. Mater. 56 (2007) 101–103.
[22] Y. Zhang, D. Kang, C. Saquing, M. Aindow, C. Erkey, Ind. Eng. Chem. Res. 44 (2005) 4161–4164.
[23] A. Smirnova, X. Dong, H. Hara, N. Sammes, J. Fuel Cell Sci. Technol. 3 (2006) 477–481.
[24] Y. Zhang, D. Kang, M. Aindow, C. Erkey, J. Phys. Chem. B 109 (2005) 2617–2624.
[25] C.D. Saquing, T.T. Cheng, M. Aindow, C. Erkey, J. Phys. Chem. B 108 (2004) 7716–7722.
[26] C.D. Saquing, D. Kang, M. Aindow, C. Erkey, Micropor. Mesopor. Mater. 80 (2005) 11–23.
[27] H.A. Gasteiger, J.E. Panels, S.G. Yan, J. Power Sources 127 (2004) 162–171.
[28] A. Smirnova, X. Dong, H. Hara, A. Vasiliev, N. Sammes, Int. J. Hydrogen Energy 30 (2005) 149–158.
[29] M. Kruk, M. Jaroniec, Y. Bereznitzki, J. Colloid Interface Sci. 182 (1996) 282–286.
[30] Z.W. Zhao, Z.P. Guo, J. Ding, D. Wexler, Z.F. Ma, D.Y. Zhang, H.K. Liu, Electrochem. Commun. 8 (2006) 245–250.
[31] A. Pozio, M.D.E. Francesco, A. Cemmi, F. Cardellini, L. Giorgi, J. Power Sources 105 (2002) 13–19.
[32] F. Gloaguen, J.M. Leger, C. Lamy, J. Appl. Electrochem. 27 (1997) 1052–1060.
[33] J. Shan, P.G. Pickup, Electrochem. Acta 46 (2000) 119–125.
[34] K. Suárez-Alcantara, A. Rodríguez-Castellanos, R. Dante, O. Solorza-Feria, J. Power Sources 157 (2006) 114–120.
[35] M. Bron, S. Fiechter, M. Hilgendorff, P. Bogdanoff, J. Appl. Chem. 32 (2002) 211–216.
[36] R. González-Cruz, O. Solorza-Feria, J. Solid State Electrochem. 7 (2003) 289–295.
[37] F. Dundar, A. Smirnova, X. Dong, A. Ata, N. Sammes, J. Fuel Cell Sci. Technol. 3 (2006) 428–433.
[38] S.K. Zečević, J.S. Wainright, M.H.S Litt, L.J. Gojković, R.F. Savinell, J. Electrochem. Soc. 144 (1997) 2973–2982.
[39] S.K. Zečević, J.S. Wainright, M.H.S Litt, L.J. Gojković, R.F. Savinell, J. Electrochem. Soc. 144 (1997) 2973–2982.
[40] R.M.Q. Mello, E.A. Ticianelli, Electrochim. Acta 42 (1997) 1031–1039.
[41] N.M. Marković, T.J. Schmidt, V. Stamenković, P.N. Ross, Fuel Cells 1 (2001) 105–116.
[42] O. Antoine, Y. Bultel, R. Durand, J. Electroanal. Chem. 499 (2001) 85–94.
[43] E.H. Yu, K. Scott, R.W. Reeve, Fuel Cells 3 (2003) 169–176.
[44] E. Antolini, L. Giorgi, A. Pozio, E. Passalacqua, J. Power Sources 77 (1999) 136–142.
[45] J. Jiang, B. Yi, J. Electroanal. Chem. 577 (2005) 107–115.